AD-A163 165 PREDICTION OF TURBULENT SKIN FRICTION FOR TWO-DIMENSIONAL RIB-TYPE SURFAC..(U) MISSISSIPPI STATE UNIV MISSISSIPPI STATE ENGINEERING INDUSTRI.. 1/1

UNCLASSIFIED R P TAYLOR ET AL. SEP 85 TFD-85-1 F/G 20/4 NL

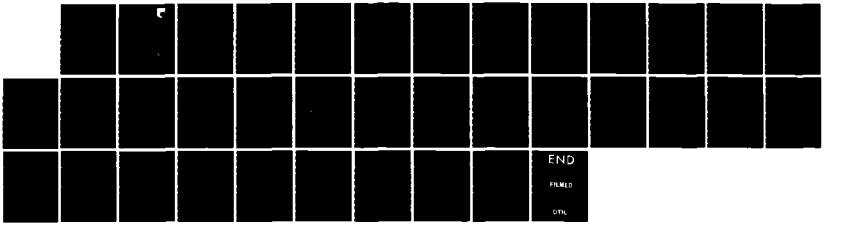

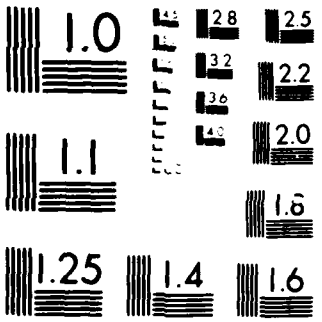
1.0
1.1
1.25
1.4
1.6
2.8
3.2
3.6
4.0
2.5
2.2
2.0
1.8

AFWAL-TR-85-3091

PREDICTION OF TURBULENT SKIN FRICTION FOR TWO-DIMENSIONAL, RIB-TYPE SURFACE ROUGHNESS USING A DISCRETE ELEMENT APPROACH

Robert P. Taylor
B. K. Hodge
Hugh W. Coleman
Mechanical and Nuclear Engineering Department
Mississippi State University
Mississippi State, MS 39762

September 1985

Final Report for Period May 1984-August 1985

FLIGHT DYNAMICS LABORATORY
AIR FORCE WRIGHT AERONAUTICAL LABORATORIES
AIR FORCE SYSTEMS COMMAND
WRIGHT-PATTERSON AIR FORCE BASE, OHIO 45433-6533

NOTICE

When Government drawings, specifications, or other data are used for any purpose other than in connection with a definitely related Government procurement operation, the United States Government thereby incurs no responsibility nor any obligation whatsoever; and the fact that the Government may have formulated, furnished, or in any way supplied the said drawings, specifications, or other data, is not to be regarded by implication or otherwise as in any manner licensing the holder or any other person or corporation, or conveying any rights or permission to manufacture, use, or sell any potential invention that may in any way be related thereto.

This report has been reviewed by the Office of Public Affairs (ASD/PA) and is releasable to the National Technical Information Service (NTIS). At NTIS, it will be available to the general public, including foreign nations.

This technical report has been reviewed and is approved for publication.

Melvin L Buck

MELVIN L. BUCK
Project Engineer

FOR THE COMMANDER

Donald A Dreesbach

DONALD A. DREESBACH, COL, USAF
Chief, Aeromechanics Division

"If your address has changed, if you wish to be removed from our mailing list, or if the addressee is no longer employed by your organization, please notify AFWAL/FIMG, W-PAFB, OH 45433 to help us maintain a current mailing list."

Copies of this report should not be returned unless return is required by security considerations, contractual obligations, or notice on a specific document.

UNCLASSIFIED

SECURITY CLASSIFICATION OF THIS PAGE

AD-A163 165

REPORT DOCUMENTATION PAGE

1a. REPORT SECURITY CLASSIFICATION	1b. RESTRICTIVE MARKINGS
2a. SECURITY CLASSIFICATION AUTHORITY	3. DISTRIBUTION/AVAILABILITY OF REPORT: Approved for public release; distribution unlimited.
2b. DECLASSIFICATION/DOWNGRADING SCHEDULE	
4. PERFORMING ORGANIZATION REPORT NUMBER(S): TFD-85-1	5. MONITORING ORGANIZATION REPORT NUMBER(S): AFWAL-TR-85-3091
6a. NAME OF PERFORMING ORGANIZATION: Mississippi State University Engr. & Indus. Research Sta. Mechanical and Nuclear Engineering Department; 6b. OFFICE SYMBOL (If applicable)	7a. NAME OF MONITORING ORGANIZATION: Flight Dynamics Laboratory (AFWAL/FIMG) Air Force Wright Aeronautical Laboratories
6c. ADDRESS (City, State and ZIP Code): P. O. Drawer ME, Mississippi State, MS 39762	7b. ADDRESS (City, State and ZIP Code): Wright-Patterson Air Force Base, OH 45433
8a. NAME OF FUNDING/SPONSORING ORGANIZATION; 8b. OFFICE SYMBOL (If applicable): FIMG	9. PROCUREMENT INSTRUMENT IDENTIFICATION NUMBER: F33615-84-K-3014
8c. ADDRESS (City, State and ZIP Code): AFWAL/FIMG, Wright-Patterson Air Force Base, OH 45433	10. SOURCE OF FUNDING NOS.

PROGRAM ELEMENT NO.	PROJECT NO.	TASK NO.	WORK UNIT NO.
61102F	2307	N4	58

11. TITLE (Include Security Classification): (see back of this form)

12. PERSONAL AUTHOR(S): Taylor, Robert P.; Hodge, B. K.; Coleman, Hugh W.

13a. TYPE OF REPORT	13b. TIME COVERED	14. DATE OF REPORT (Yr., Mo., Day)	15. PAGE COUNT
Final	FROM May 84 TO Aug 85	1985, September	25

16. SUPPLEMENTARY NOTATION

17 COSATI CODES		
FIELD	GROUP	SUB GR
01	01, 02	

18. SUBJECT TERMS (Continue on reverse if necessary and identify by block number): Two-Dimensional Roughness, Turbulent Flow, Rib Roughness, Boundary Layer, Discrete Element

19. ABSTRACT (Continue on reverse if necessary and identify by block number)

A discrete element model for turbulent flow over two-dimensional rib-type roughness is developed and validated. Surface roughness blockage effects and form drag are included as a constituent part of the differential equations. Separation and reattachment of the flow over rib roughness are identified as the dominant flow phenomena, and models are developed which incorporate the separated region geometry into the blockage. The form drag model is based on the pressure difference between the windward and leeward forces of the roughness. Predictions are compared with a variety of data sets. These comparisons indicate that the discrete element approach can be successfully applied for rib-type roughness. However, the model has a more narrow range of application for different surface geometries than the very broad range which has previously been demonstrated for three-dimensional, distributed roughness.

20. DISTRIBUTION/AVAILABILITY OF ABSTRACT	21. ABSTRACT SECURITY CLASSIFICATION
UNCLASSIFIED/UNLIMITED ☒ SAME AS RPT ☐ DTIC USERS ☐	Unclassified

22a. NAME OF RESPONSIBLE INDIVIDUAL	22b. TELEPHONE NUMBER (Include Area Code)	22c. OFFICE SYMBOL
Mel Buck	(513) 255-6156	AFWAL/FIMG

DD FORM 1473, 83 APR EDITION OF 1 JAN 73 IS OBSOLETE

UNCLASSIFIED

SECURITY CLASSIFICATION OF THIS PAGE

11. Title:

Prediction of Turbulent Skin Friction for Two-Dimensional, Rib-Type Surface Roughness Using a Discrete Element Approach

PREFACE

This program was conducted by the Mississippi State University Engineering and Industrial Research Station, P. O. Drawer ME, Mississippi State, Mississippi 39762 under Contract F33615-84-K-3014 and Modification P00003 with the Air Force Wright Aeronautical Laboratories, Wright-Patterson Air Force Base, Ohio 45433-6553. Mr. Melvin L. Buck (FIMG) managed the program for the Air Force Wright Aeronautical Laboratories. That part of the program with which this report is concerned was conducted from May 1984 to August 1985.

The authors wish to thank Mr. Melvin Buck and Dr. Tony Fiore for their support and encouragement and the Ballistic Missile Organization for their financial support.

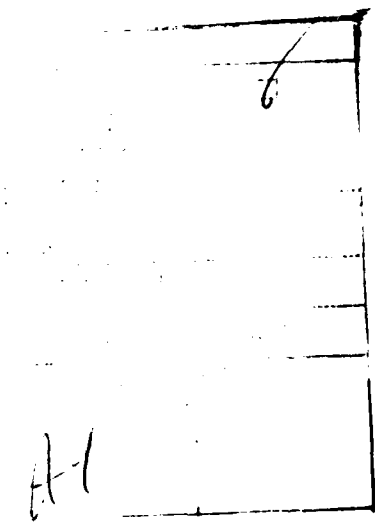

TABLE OF CONTENTS

LIST OF FIGURES

NOMENCLATURE

A^+	Van Driest damping factor = 26
A_p	Projected area of roughness element
A_s	Windward surface area of roughness element
A_x	Control surface area normal to x-axis which is open to flow
A_y	Control surface area normal to y-axis which is open to flow
C_D	Local element drag coefficient
C_{DO}	Constant in equation 9
C_f	Skin friction coefficient; defined in equation 5
D	Pipe diameter
D_h	Hydraulic diameter
d	Effective element width; defined in Figure 5a
k	Roughness element height; defined in Figure 5a
k_a	Nominal roughness height; used in Figure 1
k_s	Equivalent sand-grain roughness
L	Roughness spacing; defined in F gure 5a
ℓ_m	Mixing length; defined in equation 11
ℓ_r	Average roughness spacing; used in Figure 1
P	Pressure
U	Mean velocity component in the x-direction
V	Mean velocity component in y-direction
w	Roughness element width; defined in Figure 5a
x	Streamwise coordinate
y	Normal coordinate
y^+	Nondimensional y; $y\sqrt{\tau_w/\rho}/\nu$
z	Transverse coordinate

Greek

β_x	Blockage factor for surface normal to x-direction; defined by equation 6
β_y	Blockage factor for surface normal to y-direction
γ	Leeward separation parameter; defined in Figure 5a
Δ	Effective wall location; defined in Figure 5b
ΔP	Pressure difference

δ	Boundary layer thickness
δx	Control volume dimension; Figure 2
δy	Control volume dimension; Figure 2
Λ	Roughness density factor; used in Figure 1
μ	Viscosity
ν	Kinematic viscosity
ρ	Density
τ	Shear stress

Subscripts

e	Values at the boundary layer edge
T	Turbulent value
w	Values at the wall

SECTION I

INTRODUCTION

Skin friction can be significantly larger for turbulent flow over a rough surface as compared with an equivalent flow over a smooth surface. Many systems of engineering interest, such as re-entry vehicles, heat exchangers, aircraft, turoines and piping networks, have surfaces which are often rough in the aerodynamic or hydraulic sense. Therefore, there is significant interest in accurate predictive models for turbulent flows over rough surfaces.

In turbulent flow analysis, use of time-averaged equations leads to the necessity of formulating a turbulence model with empirical input to achieve closure. A similar situation exist in the analysis of flow over rough surfaces. Unless the equations can be solved in a grid that is fine enough to resolve the surface roughness geometry, a roughness model with empirical input is necessary.

When considering the development of predictive models for turbulent flow over rough surfaces, it is necessary to divide the surfaces into two broad classes based on the geometry of the roughness elements. These two classes are three-dimensional distributed roughness and two-dimensional rib-type roughness. The distributed roughness is, as its name implies, composed of a collection of small, mostly three-dimensional protrusions such as an array of hemispheres or the texture of a casting. Likewise, rib-type roughness is composed of two-dimensional strips, such as in a fiber-reinforced composite. While related, the interactions of these two classes of roughness with the flow field involve different physical behaviors and require separate treatments.

This report presents a discrete element model for turbulent flow over rib-type roughness. A brief discussion of the background of roughness modeling is given below and is followed by a description of the current model and comparisons of this model with experimental data sets. A more detailed discussion of roughness modeling can be found in Reference 1.

SECTION II

BACKGROUND OF ROUGHNESS MODELING

The first in-depth treatments of the effects of surface roughness on fluid flow were those of Nikuradse [2] and Schlichting [3]. Schlichting proposed that rough surfaces be classified based on equivalent sand-grain roughness (k_s). He defined k_s as the size of sand grain in Nikuradse's pipe flow experiment which would give the same skin friction as that observed on a particular rough surface, and he experimentally determined k_s for a variety of surfaces. Schlichting's work was for many years the accepted standard, and much of the subsequent theoretical and experimental research incorporated his results, explicitly or implicitly, into models and phenomenological explanations. Because Schlichting's data reduction method was flawed (mainly by neglecting the effects of the side walls on his 4:1 aspect ratio channel), much of the subsequent work which referenced his results and attempted to cast various roughnesses in terms of sand-grain equivalent are also in error. Coleman et al. [4] reported the flaw in Schlichting's data reduction procedure and presented corrected values for his data.

However, even with a consistent data base, problems remain when attempts are made to extend the sand-grain roughness concept to specific roughness geometries. Implicit in the proper use of equivalent sand-grain roughness are the dual assumptions: (1) roughness effects can be adequately described by a single parameter and (2) over a wide range of conditions the roughness behaves as if it were sand grain. As Reynolds [5] points out these are not viable assumptions for many roughness configurations. Another problem with this approach is how to determine k_s when no skin friction data exist for a particular surface.

The typical tactic taken is to try to relate k_s to geometrical attributes of a specific roughness through a correlation. Dvorak [6], Simpson [7] and Dirling [8] have presented k_s/k_a as a function of various geometrical parameters. In these correlations, k_s is the equivalent sand-grain roughness, and k_a is the nominal roughness height. These correlations do not correlate the data well, and they

rely primarily on Schlichting's results which the authors have shown to be in error [4]. Figure 1 presents the correlation of Dirling along with the original data he used. In this figure, Λ is the roughness density parameter, A_S and A_p are the windward roughness element surface area and the projected windward surface area respectively, and ℓ_r is the average center-to-center spacing. While the Dirling correlation tends to yield the correct trends, the scatter is quite severe as k_s/k_a varies by a factor of three-to-four for most Λ values. Berg [9], for example, found that the Dirling correlation gave a k_s/k_a value three times larger than his experimentally determined values.

The correlation also treats two-dimensional and three-dimensional roughness in the same manner, even though the nature of the flow around the two types is very different. This is evident also from Figure 1, where, except for the most densely packed spherical roughness elements of Schlichting, the two- and three-dimensional roughness correlations are distinct. The flow over two-dimensional elements is primarily dependent on the spacing/height ratio whereas spacing, shapes and height are all important for flow over and around three-dimensional elements. Perry et al. [10] found that for transverse bar elements with certain height-to-spacing ratios the skin friction does not scale with the roughness height. The k_s concept is particularly poor for rib-type roughness. Morris [11] presented a classification of rib-type roughness which was based primarily on the rib spacing to height ratio (L/k). Reynolds [5] identified four distinct relationships of skin friction with Reynolds number, only one of which is "sand grain" in behavior. Several correlations for friction coefficient have been presented based on the [illegible] of equivalent sand-grain roughness (Han et al. [illegible], for example.

Because of the restrictive nature of the implications of basing [illegible] on sand grain or equivalent sand-grain roughness concepts, the more fundamentally based discrete element roughness model was chosen. This approach models the interaction of the roughness and the flow by accounting for the blockage effect of the roughness and the drag force which the roughness elements exert

on the fluid. Roberson and his co-workers (Reference 13, for example) used some aspects of this model in their insightful work. Finson [14], Lin and Bywater [15] and Christoph and Pletcher [16] have reported work which uses these concepts. The most recent results have been presented by the authors [1, 17]. The discrete element roughness model for rib-type roughness is examined in the next section.

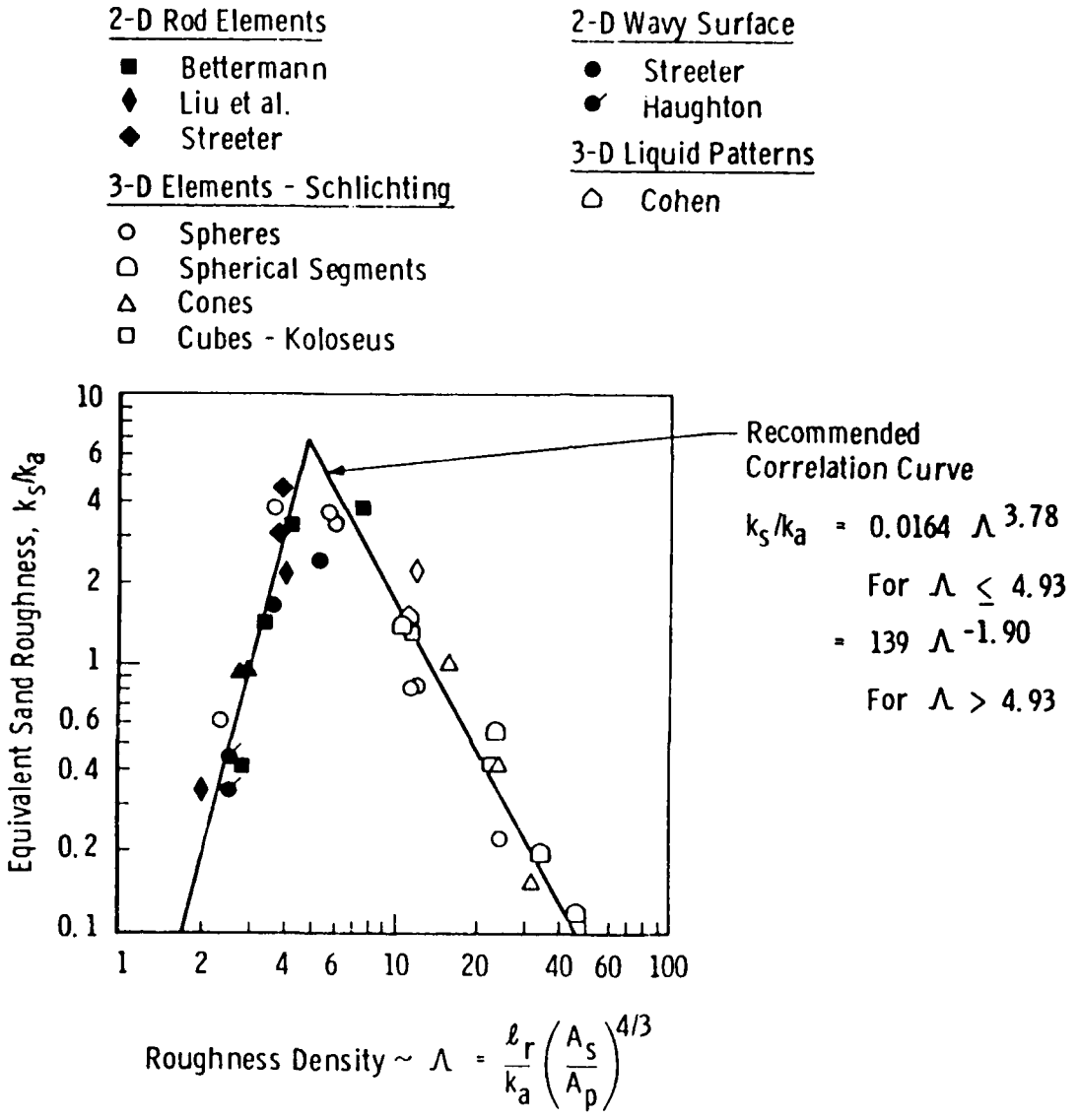

Figure 1. Effective Sand-Grain Roughness Correlation of Dirling [8]

SECTION III

DISCRETE ELEMENT MODEL FOR RIB-TYPE ROUGHNESS

It has long been recognized that the governing phenomenon of the interaction between rib roughness and the flow is the momentum sink, which results in the form drag of the roughness. Morris [11] suggested that form drag concepts could be used to predict the friction factor for flow over rib-type roughness. Lewis [18] used these ideas as a tool in the interpretation of his experimental data. However, a complete discrete element formulation has not been used to predict the turbulent flow field over surfaces with rib-type roughness.

The discrete element approach considers the mass and momentum transport processes on the collection of individual roughness elements and the smooth surface between them. The basic idea of the discrete element approach is to formulate a system of partial differential equations which describe the mass and momentum transport over and between the elements. In this method the roughness effects (form drag and blockage) are taken as an integral part of the problem.

The development and validation of the discrete element roughness model of Coleman et al. is discussed in detail in References 1 and 17. An abbreviated discussion is presented herein. In the discrete element approach the rough surface is assumed to be composed of distinct roughness elements. This model is based on consideration of the physics of the interactions between the discrete roughness elements and the flow and does not depend on the assumption of any sand-grain roughness equivalent. An array of two-dimensional roughness elements perpendicular to the streamwise direction, x, is used in the following discussion.

The differential equations including roughness effects are derived by applying the basic conservation statements for mass and momentum to a control volume (CV) such as that shown in Figure 2. This CV is shown with an exaggerated length, δx, in the primary flow

direction as an aid in correctly formulating the roughness effects. The CV includes all the fluid in the volume and, as shown, is

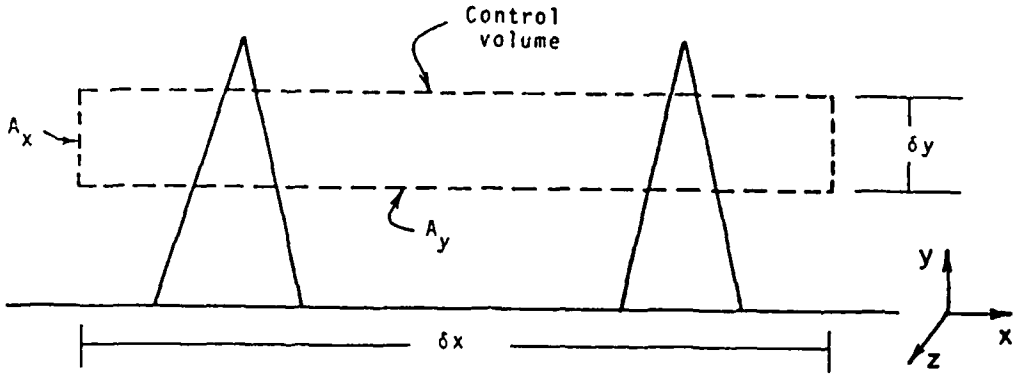

Figure 2. Control Volume for Flow Over Two-Dimensional Roughness

penetrated by roughness elements. The physical effects of the roughness elements on the fluid in the CV are modeled by considering the flow blockage and by postulating that the total force of the elements on the flow can be incorporated as a drag force.

Basic to this approach is the idea that the two-dimensional, time-averaged turbulent boundary layer equations can be applied in the flow region below the crests of the roughness elements. Therefore, the flow variables must be viewed as having been averaged over the transverse (z) direction and averaged in the longitudinal (x) direction over an appropriate x distance.

Mass and momentum balances were made for this control volume in order to derive the partial differential equations that describe the flow over a rough surface. The resulting partial differential equations were then time averaged (Reynolds averaged) and the boundary-layer assumptions invoked. The resulting equations are

Continuity

$$\frac{\partial}{\partial x}(\rho\beta_x U) + \frac{\partial}{\partial y}(\rho\beta_y V) = 0 \qquad (1)$$

x-Momentum

$$\rho\beta_x U \frac{\partial U}{\partial x} + \rho\beta_y V \frac{\partial U}{\partial y} = \rho_e \beta_x U_e \frac{dU_e}{dx}$$

$$+ \frac{\partial}{\partial y}\left[\beta_y(\mu + \mu_T)\frac{\partial U}{\partial y}\right] \qquad (2)$$

$$- \frac{1}{2}\rho C_D \frac{1}{L} U^2$$

and the associated boundary conditions are

$$y = 0 \; : \; U = V = 0 \qquad (3)$$

$$y \to \infty \; : \; U \to U_e \qquad (4)$$

where β_x and β_y are the blockage factors, L is the distance between ribs and C_D is the local element drag coefficient.

A comparison of the above equations with the standard time-averaged turbulent boundary-layer equations for smooth walls reveals the results of including the discrete roughness elements. A term-by-term examination of the differences is appropriate. The parameter β represents the fraction of the control surface (CS) open to the flow. β_x is the fraction of the CS perpendicular to the x-coordinate that is open to the flow; β_y is the fraction of the CS perpendicular to the y-coordinate that is open to the flow. β_x and β_y, the blockage factors, also appear in the x-momentum equation. The additional term in the x-momentum equation represents the form drag of the roughness elements and is represented in terms of a drag coefficient. This term acts as a distributed momentum sink.

The skin friction coefficient for the discrete roughness element model is as follows:

$$C_f = \frac{(\beta_x)_w \tau_w + \frac{1}{2}\frac{1}{L}\int_o^\infty \rho C_D U^2 (dy)}{\frac{1}{2}\rho U_e{}^2} \qquad (5)$$

The subscript w indicates values evaluated at the wall, and the e indicates boundary-layer edge conditions. The smooth wall shear stress τ_w is given by $\mu(\partial U/\partial y)_w$. The skin friction coefficient is a non-dimensionalized form of the apparent wall shear stress. The

apparent wall shear stress is composed of the viscous shear term acting over the portion of the wall not occupied by roughness elements (the smooth portion) plus the resultant form drag on the rib roughness elements. The proper formulations for the blockage factors, β_x and β_y, and the drag coefficient, C_D, along with turbulent closure, complete the model.

SECTION IV

ROUGHNESS MODEL FOR RIB-TYPE ROUGHNESS

For three-dimensional roughness, the blockage factors required for the discrete element model of Coleman et al. [1, 17] were functions of only the roughness element geometry. However, the blockage factors for the discrete element formulation for two-dimensional, rib-type roughness require some fluid mechanical considerations.

Figure 3, taken from Lewis [18], provides a phenomenological schematic of the salient features of the interaction of rib-type roughness and the turbulent boundary layer in which it is immersed.

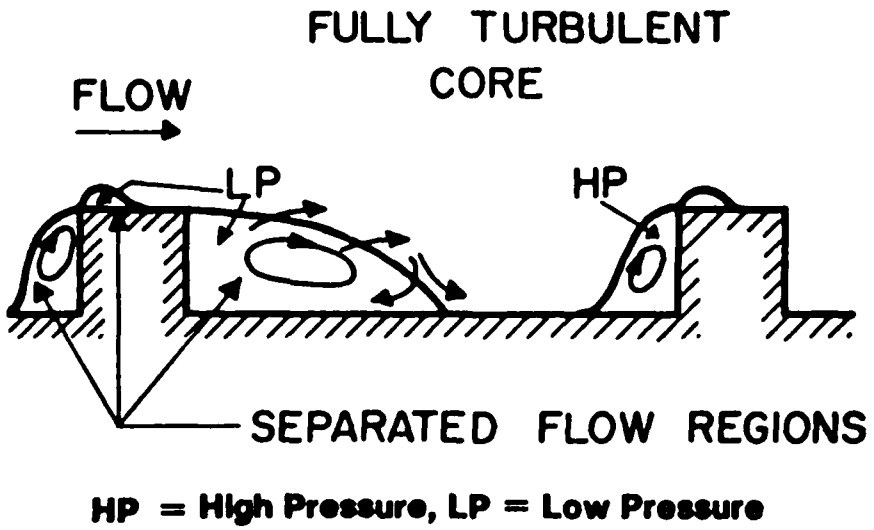

Figure 3. Schematic of Salient Features of Flow Over Two-Dimensional Roughness (From Lewis [18])

The dominant features of the interaction are flow separation and reattachment. These regions of separated flow give rise to a momentum sink which results in the form drag of the element. Three separated regions are present on a given rib: (1) a large (in comparison to the rib size) region downstream of the element, (2) a smaller region over the upstream face of the element, and (3) a very

small (in comparison to the rib size) region on the upstream side of the top of the element. The windward (upstream) face sees a much higher pressure level than the leeward (downstream) face.

If the rib spacing is large enough, the boundary layer reattaches to the wall at some point between the ribs. The quantitative aspects of these separations and reattachments are highly dependent upon the rib geometry and attributes of the turbulent boundary layer. In situations where the streamwise flow reattaches to the wall, the streamlines drop below the crests of the two-dimensional ribs and then move above the crests in the neighborhood of the following elements.

Quantitative details in the form of static pressure isobars for the flow field over a square-rib configuration are presented in Figure 4. This figure was taken from Lawn [19] and is illustrative

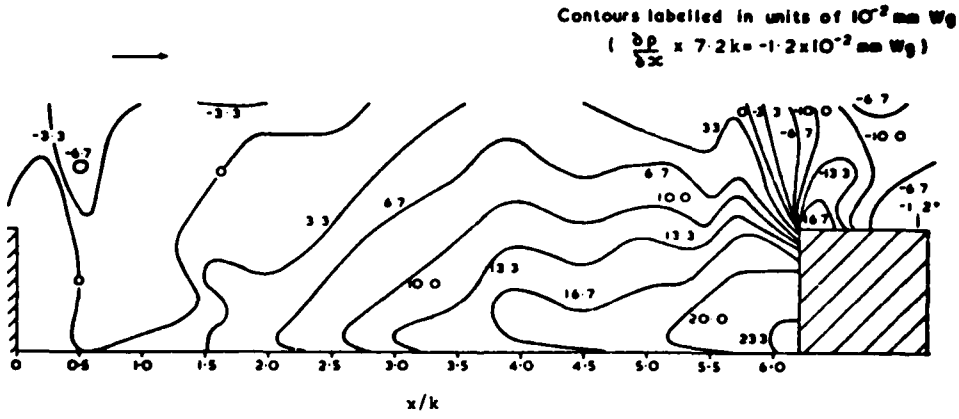

Figure 4. Isobars of Typical Flow Over Two-Dimensional Rib Roughness (from Lawn [19])

of the comp' xity of the flow structure encountered in turbulent boundary layer flow over two-dimensional roughness configurations. The pressure variation over the upstream face of the element shows a decrease from the base of the element to the top of the element; whereas the pressure on the rear face (downstream side) of the element is at a much lower level and is essentially constant.

The information presented in Figures 3 and 4 is indicative of the complexity of the viscous flow over two-dimensional roughness. The presence of the boundary layer is responsible for much of the complexity. Good and Joubert [20] point out that while bluff bodies immersed in an external flow have essentially a constant form-drag coefficient (for all Reynolds numbers above a few thousand), bluff bodies immersed in a turbulent boundary layer have form-drag coefficients that are dependent upon the Reynolds number because of the distribution of the incident momentum flux and the behavior of the separated regions.

If the flow about two-dimensional rib roughness is to be calculated in detail, then the Navier-Stokes equations with an appropriate grid and turbulence model must be used. For roughnesses with small spacings, a grid system which resolves the surface geometry presents a difficult problem. Indeed, the complexity of the physics of the rib roughness/turbulent boundary layer interaction is so great that only recently have turbulence models and numerical techniques been developed that can adequately predict important features of the flow. The recent work of Benodekar et al. [21] using a modified two-equation (κ, ε) turbulence model is typical of recent (1985) predictive efforts. While they predicted important nuances of some characteristics of the flow field over a single rib element, some anomalies were present. For example, the predictions of the upstream pressure rise were in excellent agreement with the data, but the prediction of the downstream pressure variation showed some discrepancies. The predicted velocity profiles were not in agreement with measured profiles downstream of the roughness element.

The preceding background information is sufficient to develop the roughness model. Equations (1) and (2) were obtained by averaging the effects of roughness in the longitudinal (x) and transverse (z) directions. Thus, the blockage terms and the form drag (momentum sink) expression, as they appear in equations (1) and (2), are in effect expressed on a per unit length basis in the streamwise direction. Hence the discrete element roughness model for two-dimensional, rib-type roughness makes no attempt to model details of the flow field at discrete roughness locations, but instead models

the effects of blockage and form drag in such a manner that the average wall resistance (viscous shear plus form drag) is accurately predicted. The regions of separation, which would require Navier-Stokes computations, are replaced by the roughness model so that parabolic (marching) computational techniques with the turbulent boundary layer equations can be utilized.

In a manner similar to that of Morris [11], the flow over rib-type roughness is divided into three regimes:

1) Reattached flow - the separated region behind the rib reattaches to the smooth surface between the ribs; viscous skin friction is a significant factor.
2) Unreattached flow - the separated regions behind and in front of the ribs merge; viscous skin friction is relatively unimportant.
3) Skimming flow - the region between the ribs is completely filled with a recirculating flow, the surface appears semi-smooth.

The formulation presented herein applies only to regimes 1 and 2. Figure 5a and 5b schematically illustrate the models for these regimes. The separated region upstream of the roughness is taken to be the same length as the element height. This agrees qualitatively with the interaction given by Lawn [19] and presented in Figure 4, and with the suggestion of Lewis [18]. For the purposes of blockage factor calculations, the separated region is taken to be that area enclosed by a line extending from the separation location to the tip of the element.

The downstream separation length is taken as Yk and will be discussed in more detail later. Similar to the upstream region, the downstream separated region is taken as extending from the tip of the roughness element to the reattachment point. The factor β is defined as that fraction of a control surface that is open to flow and the action of viscous shear due to attached streamwise flow. The large separated regions before and after the rib act as blockage to the main flow field. Referring to Figure 5a the blockage factor for an

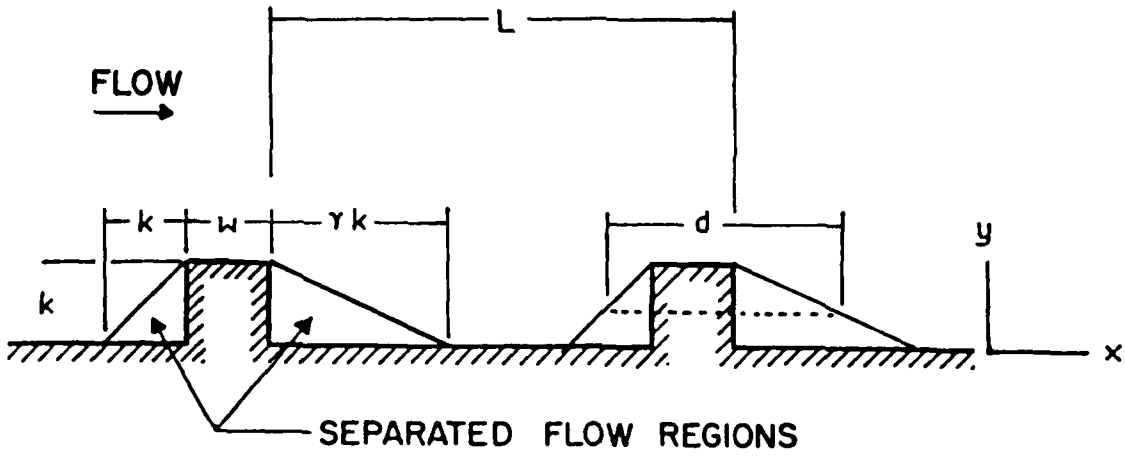

(a) Reattached Flow

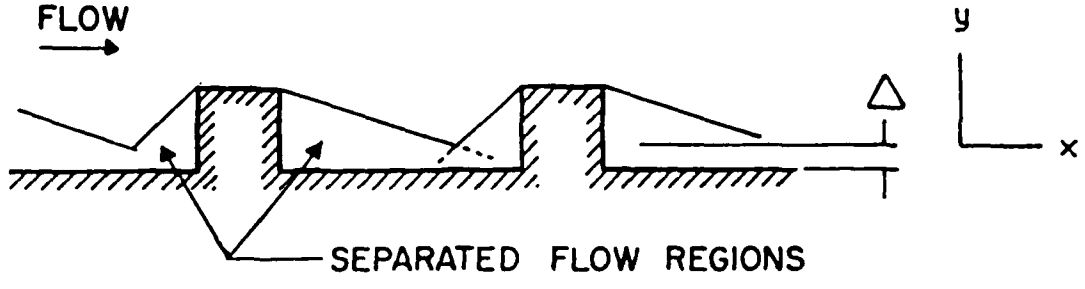

(b) Unreattached Flow

Figure 5. Schematic of Blockage Model for Two-Dimensional Roughness

x-z plane is seen to be

$$\beta_y = 1 - d/L \tag{6}$$

where $d = w + (\gamma + 1)(k - y)$

The blockage factor for the y-z plane, β_x, is more difficult to define. For some y-z planes the flow is completely blocked below the crest of the ribs. For others there is no blockage. If an average is taken over a length containing several ribs, an average blockage factor in y-z planes is found which is approximately equal to the x-z blockage factor given in equation (6). Above the ribs the blockage factor is 1 for both β_x and β_y.

For flow where the separated regions merge, regime 2, the same equations apply. However, since the wall is completely covered by the recirculating flow, a new origin for y must be taken. Referring to Figure 5b and following Lewis [18], the new origin is located a distance Δ above the base wall where

$$\Delta = k - (L - w)/(\gamma + 1) \tag{7}$$

The effect of this construction is to treat the roughness as shorter ribs in regime 2 flows.

As shown by the data of Lawn [19] and presented in Figure 4, the fluid flowing over the roughness ribs results in nearly constant pressure on the leeward side of a rib. The pressure on the windward side decreases from the base to the top of the rib. It is this windward-to-leeward side pressure difference which results in the local form drag. As shown in equation (2) this local drag force is cast in terms of a local drag coefficient

$$C_D = 2\Delta P/\rho U^2 \tag{8}$$

Since the pressure difference decreases with distance above the base wall while the velocity increases with distance above the base wall, C_D must be a decreasing function of the distance above the base surface. Based on Lawn's [19] detailed pressure and velocity distribution measurements in the neighborhood of roughness ribs, the following formulation was used

$$C_D = C_{DO}\ (1 - y/k) \tag{9}$$

The constant C_{DO} was found by calibration using comparisons of numerical experiments with base data sets.

For turbulent flow some closure model must be adopted to relate the shear stress, τ, to the mean flow field. Here the Boussinesq approximation is invoked:

$$\tau = (\mu + \mu_T) \frac{\partial U}{\partial y} \tag{10}$$

The eddy viscosity, μ_T, is modeled using the usual smooth wall Prandtl mixing-length model with van Driest damping. Since the roughness effects were incorporated entirely into the roughness model, the mixing-length model used was the conventional one used for smooth surfaces. That model is (Schetz [22])

$$\ell_m = 0.40y\left[1 - \exp(-y^+/A^+)\right] \; ; \; \ell_m < 0.09\,\delta$$

$$\ell_m = 0.09\delta \text{ otherwise.} \tag{11}$$

The appropriateness of using a smooth-wall, mixing-length model was validated by Taylor et al. [1] for three-dimensional roughness.

The time-averaged turbulent boundary-layer equations as formulated for discrete element roughness and with the aforementioned turbulence and roughness models were solved numerically using an implicit finite difference technique similar to that of Adams and Martindale [23]. Comparisons of the discrete element roughness model as developed herein with several experimental data sets are presented in the next sections.

SECTION V

COMPARISON OF PREDICTIONS WITH EXPERIMENTAL DATA

Comparisons have been made between predictions using the model described herein and several experimental data sets [12, 24, 25, 26]. The range of Reynolds numbers based on diameter or hydraulic diameter for these comparisons was approximately 6,000 to 200,000. The data show [11, 18] that the length of the leeward separated region is between 3k and 8k. For all the predictions shown in this paper $\gamma = 5$ was used. This value gave the best results for the more closely spaced rib elements, $L/k < 10$. For the more widely spaced rib elements, the model was relatively insensitive to γ within the range 3 to 8. Based on comparisons with Schlichting's [3] corrected[1] rib-roughness data, the drag coefficient function constant was initially taken to be $C_{D0} = 40$. The predictions presented in this work are all for fully developed flow between parallel plates or in pipes. The motivation for using these conditions is the great wealth of experimental data that exists for these configurations. The boundary-layer equations (1) and (2), are readily reduced for these configurations. All of the comparisons made below are for rectangular rib roughness.

Webb, Eckert and Goldstein [26] reported data for fully developed flow in square-rib-roughened pipes with a variety or rib height-to-diameter ratios, k/D, and pitch-to-height ratios, L/k. Figure 6 shows the comparison of the predictions with their data for $L/k = 10$ and $k/D = 0.01$, 0.02 and 0.04, using $C_{D0} = 40$. Inspection of the figure reveals that the agreement is good for all cases.

All of the comparisons above were for rib pitch-to-height ratios of $L/k = 10$. Webb et al. also presented data for $L/k = 20$ and $L/k = 40$. Figure 7 presents comparisons between predictions and the data. At first the same value of $C_{D0} = 40$ was used for the predictions. However, for the more widely spaced ribs this value of C_{D0} did not

---

[1]Schlichting's [3] rib-roughness data was corrected in the same manner as that reported by the authors [4] for his distributed roughness.

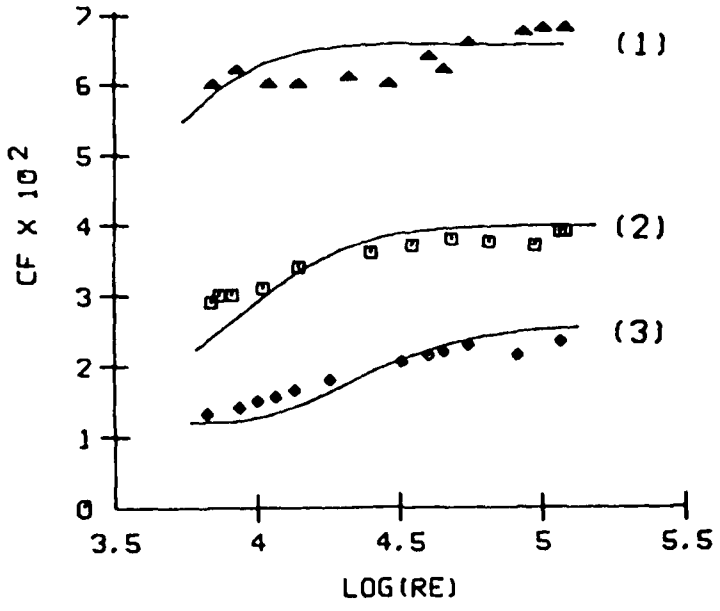

Figure 6. Comparison with Data (denoted by symbols) of Webb et al. [26] for L/k = 10; (1) k/D = 0.04; (2) k/D = 0.02; (3) k/D = 0.01; C_{DO} = 40 for all Cases

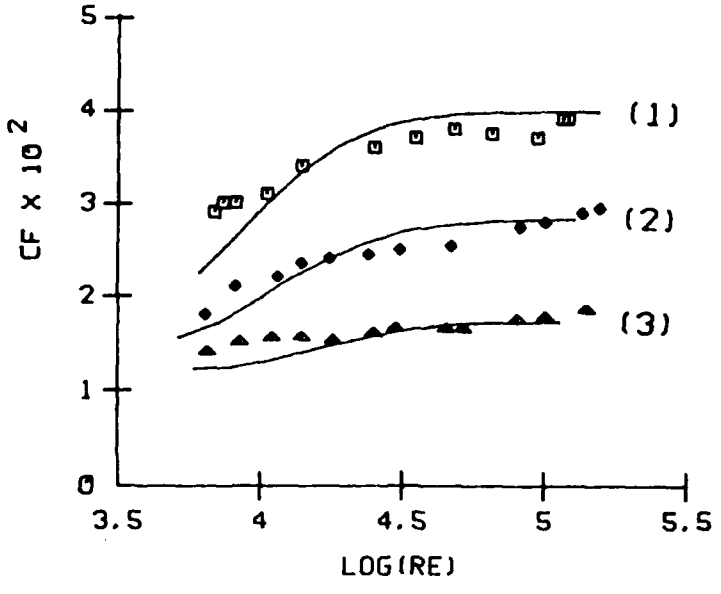

Figure 7. Comparison with Data (denoted by symbols) of Webb et al. [26] for k/D = 0.02; (1) L/k = 10, C_{DO} = 40; (2) L/k = 20, C_{DO} = 20; (3) L/k = 40, C_{DO} = 10

provide satisfactory results. As shown in the figure, a value of C_{DO} = 20 was found to give good results for L/k = 20, and a value of C_{DO} = 10 was found to give good results for L/k = 40.

Berger and Whitehead [24] presented data for fully developed flow in square rib-roughened pipes with a height-to-diameter ratio of k/D = 0.02. Pitch-to-diameter ratios of 10, 7.2, 5 and 3 were used. Figure 8 shows comparisons of predictions with these data for C_{DO} = 40. Inspection of the figure reveals that the comparison is good for the larger Reynolds numbers where C_f is essentially constant. For the more closely spaced roughness, the data show an

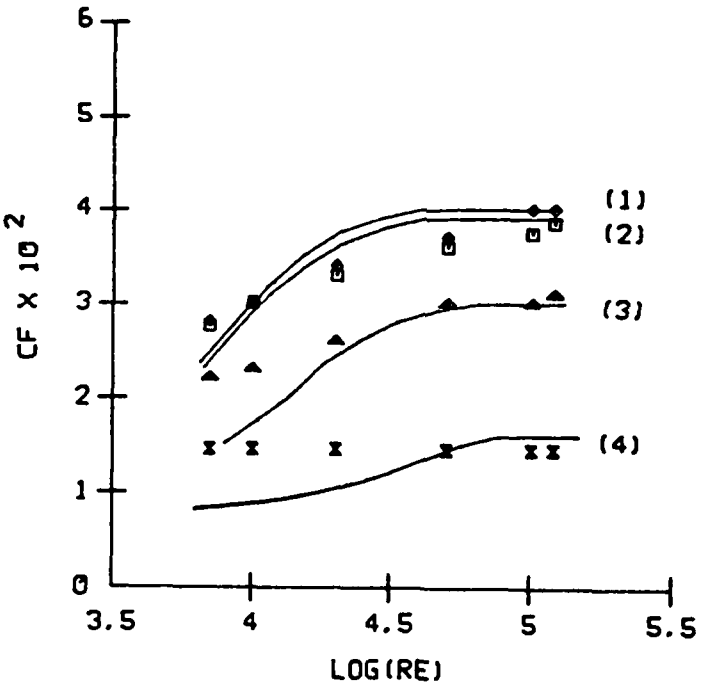

Figure 8. Comparison with Data (denoted by symbols) of Berger and Whitehead [24] for k/D = 0.02; (1) L/k = 7.2; (2) L/k = 10; (3) L/k = 5; (4) L/k = 3; C_{DO} = 40 for all Cases

almost constant C_f for all Reynolds numbers while the predictions still indicate that C_f decreases with decreasing Reynolds number. The predictions indicate the correct trends for the effect of pitch-to-height ratio. The predicted value of C_f increases as L/k increases from 3 to 7.2 and then decreases slightly for L/k = 10.

Stukel, Hopke and Nourmohammadi [25] presented data for fully developed flow in square-rib-roughened pipes for a wide variety of pitch-to-height ratios ranging from L/k = 2 to 25. The data shown in Figure 9 are for a height-to-diameter ratio of k/D = 0.072. The

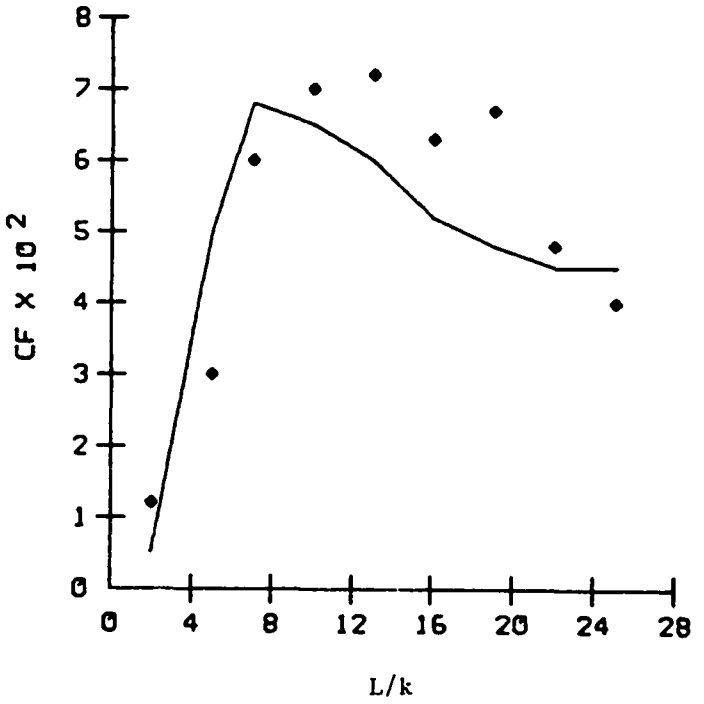

Figure 9. Comparison with Data (denoted by symbols) of Stukel et al. [25]; Re = 150,000; k/D = 0.072; C_{DO} = 10 for all Cases

value of C_{DO} used for the predictions shown was C_{DO} = 10. Inspection of the figure reveals that the model predicts the correct trends of the influence of L/k. However, the model predicts the maximum value of C_f at L/k = 8 while the data indicate a maximum near L/k = 12.

Han, Glicksman and Rohsenow [12] presented data for fully developed flow in square-rib-roughened channels with a wide variety of L/k and k/D_h values. Comparisons with selected data are shown in Figures 10 and 11. Figure 10 shows comparisons for L/k = 5 and k/D_h = 0.076 and 0.046. The value used for C_{DO} in Figure 10 was 40. From the figure it is seen that the predictions agree with the data for Reynolds numbers above approximately 10,000 where both the data and predictions shown an essentially constant value of C_f. For lower Reynolds numbers the model predicts a more rapid decrease in C_f than the data. Figure 11 shows comparisons for k/D_h = 0.056 with L/k = 10

and 20. Following the experience with the data of Webb et al. for $L/k = 10$, C_{DO} was taken to be 40; and for $L/k = 20$, C_{DO} was taken to be 20. Inspection of the figure reveals that the model overpredicts the skin friction coefficient for these data by about 20%.

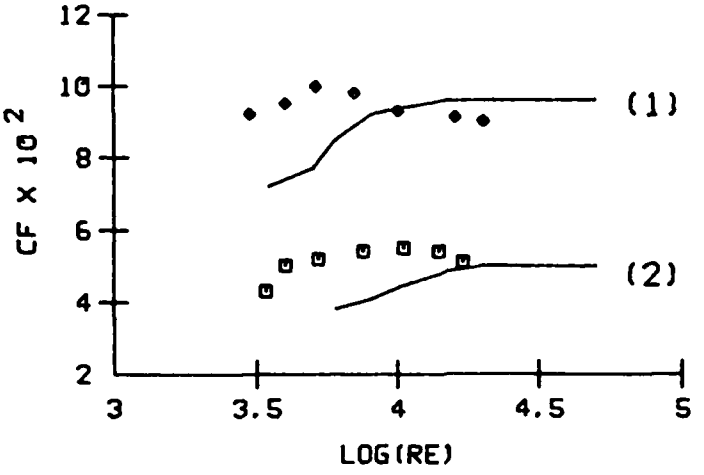

Figure 10. Comparison with Data (denoted by symbols) of Han et al. [12] for $L/k = 5$; (1) $k/D_h = 0.076$; (2) $k/D_h = 0.046$; $C_{DO} = 40$ for all Cases

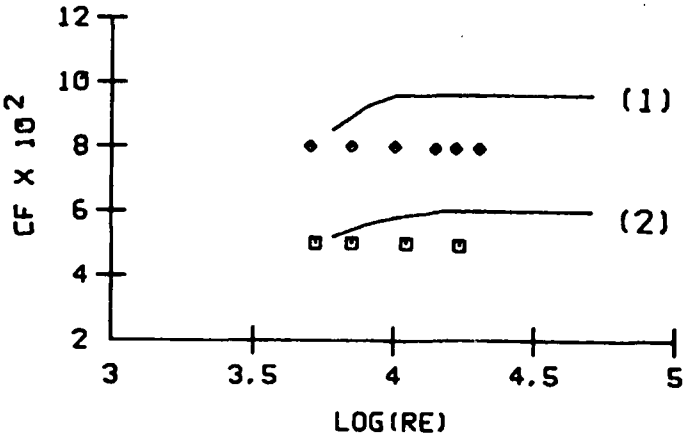

Figure 11. Comparison with Data (denoted by symbols) of Han et al. [12] for $k/D = 0.056$; (1) $L/k = 10$, $C_{DO} = 40$; (2) $L/k = 20$, $C_{DO} = 20$.

SECTION VI

DISCUSSION AND CONCLUSIONS

From the comparisons shown in the preceding section, it is seen that the model reproduces important salient features of the turbulent flow over two-dimensional rib roughness. However, it is found that the discrete element approach has a much narrower range of application for different two-dimensional surface geometries than the very broad range which has previously been demonstrated by the authors [1, 17] for three-dimensional, distributed roughness. This is shown by the necessity of changing the drag coefficient parameter, C_{DO}, for different values of L/k. This should not have been surprising since the length of attached stream-wise flow influences the shape of the upstream velocity profile (momentum distribution) which determines in part the pressure distributions on the upstream and downstream faces of a two-dimensional roughness element. The details of the nature of the windward-and-leeward separated regions and the interaction with the main streamwise flow are important in establishing the form drag of the roughness element.

Based on the comparisons with experimental data, the following values of C_{DO} are proposed:

$$C_{DO} = 40, \quad L/k \leq 10 \tag{12}$$

$$C_{DO} = 400/(L/k), \quad L/k > 10$$

This formulation gives reasonable agreement for Re > 10,000 for three of the four data sets considered. The exception is the data of Stukel et al. [25]. In this data set the rib height was 14% of the pipe radius, and the axial variation of the centerline velocity was significant between the ribs. This effect was not taken into account in this study.

Although the two-dimensional rib-roughness model developed herein was successful in predicting many important salient features of the dependence of skin friction on rib spacing, rib size, and Reynolds number, overall the model's results were not nearly as satisfying as those of the previously developed three-dimensional roughness model. With the three-dimensional distributed roughness,

the averaging processes employed in the x-z and y-z planes are physically more meaningful and appropriate than for the two-dimensional roughness.

Because equations (1) and (2) are the correct equations for discrete element considerations, any further advance in the predictive ability of the technique developed herein must come through better modeling of the blockage factors and form drag. The two-dimensional roughness elements are in discrete locations, perpendicular to the streamwise flow, and cause significant local perturbations including streamline curvature. The key to modeling two-dimensional roughness in the discrete element averaging sense is specification of the separation lengths and the form drag coefficient variation over the roughness geometry. Since the discrete element technique and two-dimensional rib-roughness models are attempts to construct a completely parabolic (marching) methodology for situations which in reality possesses significant embedded elliptic regions, one should not expect a two-dimensional boundary layer approach with any roughness model to have broad applications for turbulent flow over rib-roughened surfaces.

Another area of importance for further investigation is two-dimensional rib-roughness not oriented perpendicular to the streamwise flow. Cross flow effects for this condition are likely to be important, and the model developed herein will need further modification.

REFERENCES

1. Taylor, R. P., Coleman, H. W. and Hodge, B. K., "A Discrete Element Predictive Approach for Turbulent Flow Over Rough Surfaces," Report TFD-84-1, Mechanical and Nuclear Engineering Department, Mississippi State University, 1984.
2. Nikuradse, J., "Laws for Flows in Rough Pipes," VDI-Forchungsheft 361, Series B, Vol. 4, 1933; NACA TM 1292, 1950.
3. Schlichting, H., "Experimental Investigation of the Problem of Surface Roughness," Ingenieur-Archiv, Vol. VII, No. 1, 1936; NACA TM 823, 1937.
4. Coleman, H. W., Hodge, B. K. and Taylor, R. P., "A Re-Evaluation of Schlichting's Surface Roughness Experiment," J. Fluids Eng., Vol. 106, pp. 60-65, 1984.
5. Reynolds, A. J., Turbulent Flows in Engineering, John Wiley, New York, 1974.
6. Dvorak, F. A., "Calculation of Turbulent Boundary Layers on Rough Surfaces in Pressure Gradients," AIAA J., Vol. 7, pp. 1752-1759, 1969.
7. Simpson, R. L., "A Generalized Correlation of Roughness Density Effects on the Turbulent Boundary Layer," AIAA J., Vol. 11, pp. 242-244, 1973.
8. Dirling, R. B., Jr., "A Method for Computing Rough Wall Heat Transfer Rates on Reentry Nose Tips," AIAA Paper No. 73-763, 1973.
9. Berg, D. E., "Surface Roughness Effects on the Hypersonic Turbulent Boundary Layer," Ph.D. Dissertation, GALCIT, Cal. Tech., 1977.
10. Perry, A. E., Schofield, W. H. and Joubert, P. H., "Rough Wall Turbulent Boundary Layers," J. of Fluid Mech., Vol. 27, pp. 383-413, 1969.
11. Morris, H. M., Applied Hydraulics in Engineering, Ronald Press Co., New York, 1953.
12. Han, J. C., Glicksman, L. R. and Rohsenow, W. M., "An Investigation of Heat Transfer and Friction for Rib-Roughened Surfaces," Int. J. Heat Mass Transfer, Vol. 21, pp. 1143-1156, 1978.

13. Chen, C. K. and Roberson, J. A., "Turbulence in Wakes of Roughness Elements," J. Hydraulics Division, ASCE, Vol. 100, No. HY1, pp. 53-67, 1974.

14. Finson, M. L., "A Model for Rough Wall Turbulent Heating and Skin Friction," AIAA Paper 82-0199, 1982.

15. Lin, T. C. and Bywater, R. J., "The Evaluation of Selected Turbulence Models for High-Speed Rough-Wall Boundary Layer Calculations," AIAA Paper 80-0132, 1980.

16. Christoph, G. H. and Pletcher, R. H., "Prediction of Rough-Wall Skin Friction and Heat Transfer," AIAA J., Vol. 21, No. 4, pp. 509-515, 1983.

17. Taylor, R. P., Coleman, H. W. and Hodge, B. K., "Prediction of Turbulent Rough-Wall Skin Friction Using a Discrete Element Approach," J. Fluids Eng., Vol. 107, pp. 251-257, 1985.

18. Lewis, M. J., "An Elementary Analysis for Predicting the Momentum- and Heat-Transfer Characteristics of a Hydraulically Rough Surface," J. Heat Transfer, Vol. 97, pp. 249-254, 1975.

19. Lawn, C. J., "Flow Measurements for Establishing the Mechanisms of Heat Transfer from a Rib-Roughened Surface," Central Electricity Generating Board, Berkeley Nuclear Laboratories, Report RD/B/N3514, 1976.

20. Good, M. C. and Joubert, P. N., "The Form Drag of Two-Dimensional Bluff-Plates Immersed in Turbulent Boundary Layers," J. Fluid Mech., Vol. 31, Part 3, pp. 547-582, 1968.

21. Benodekar, R. W., Goodard, A. J. H., Gosman, A. D. and Issa, R. I., "Numerical Prediction of Turbulent Flow Over Surface-Mounted Ribs, AIAA J., Vol. 23, pp. 359-366, 1985.

22. Schetz, J. S., Foundations of Boundary Layer Theory for Momentum, Heat, and Mass Transfer, Prentice-Hall, Inc., Englewood Cliffs, NJ, 1984.

23. Adams, J. C. and Martindale, W. R., "Hypersonic Lifting Body Boundary-Layer Analysis at High Angles of Incidence," J. of Spacecraft and Rockets, Vol. 11, No. 10, p. 721, 1974.

24. Berger, F. P. and Whitehead, A. W., "Fluid Flow and Heat Transfer in Tubes with Internal Square Rib Roughening," J. Br. Nucl. Energy Soc., Vol. 16, No. 2, 1977.

25. Stukel, J. J., Hopke, P. K. and Nourmohammadi, J., "Turbulent Air Flow Over Rough Surfaces: Mean Flow Parameters," J. Fluids Eng., Vol. 106, pp. 405-409, 1984.

26. Webb, R. L., Eckert, E. R. G. and Goldstein, R. J., "Heat Transfer and Friction in Tubes with Repeated-Rib Roughness," Int. J. Heat Mass Transfer, Vol. 14, pp. 601-617, 1971.

☆ U.S. GOVERNMENT PRINTING OFFICE 646-067/10630

24. Berger, F. P. and Whitehead, A. W., "Fluid Flow and Heat Transfer in Tubes with Internal Square Rib Roughening," J. Br. Nucl. Energy Soc., Vol. 16, No. 2, 1977.

25. Stukel, J. J., Hopke, P. K. and Nourmohammadi, J., "Turbulent Air Flow Over Rough Surfaces: Mean Flow Parameters," J. Fluids Eng., Vol. 106, pp. 405-409, 1984.

26. Webb, R. L., Eckert, E. R. G. and Goldstein, R. J., "Heat Transfer and Friction in Tubes with Repeated-Rib Roughness," Int. J. Heat Mass Transfer, Vol. 14, pp. 601-617, 1971.

☆ U.S. GOVERNMENT PRINTING OFFICE 646-067 10630

END

FILMED

3-86

DTIC